Pedobarographic Statistical Parametric Mapping of plantar pressure data in new and confident walking infants: a preliminary analysis

Eleonora Montagnani[A*], Stewart C Morrison[A], Matyas Varga[A], Carina Price[B]

[A] School of Health Sciences, University of Brighton, Darley Road, Eastbourne, United Kingdom

[B] Centre for Health Sciences Research, University of Salford, Frederick Road, Salford, United Kingdom

***Corresponding author:**

Eleonora Montagnani

Email: e.montagnani@brighton.ac.uk

Address: 204 Aldro Building, 49 Darley Road, Eastbourne, BN20 7UR, UK

Word count of the manuscript (without reference list): 3163 words

Abstract

In infancy, plantar pressure data during walking has been investigated through regional approaches, whilst the use pedobarographic Statistical Parametric Mapping (pSPM) has not been reported. Analysis of pressure data using pSPM is higher in resolution and can enhance understanding of foot function development, providing novel insights into plantar pressure changes. This work aims to detail the implementation of the pSPM data processing framework on infants' pressure data, comparing plantar pressure patterns between new and confident walking steps. Twelve infants walked across an EMED-xl platform. Steps were extracted and imported into MATLAB for analysis. Maximum pressure pictures were transformed to point clouds and registered within and between participants with iterative closest point and coherent point drift algorithms, respectively. Root mean square error (RMSE) was calculated within both registrations as a quality measure. Pressure patterns were compared between new and confident walking using nonparametric-paired sample SPM1D t-test. RMSEs were under 1 mm for both registration algorithms. In the transition to confident walking, significantly increasing pressure was detected in the left central forefoot. Implementing pSPM to infants' pressure data was non-trivial, as several phases of data processing were required to ensure a robust approach. Our analysis highlighted the presence of significant changes in pressure in central left forefoot after 2.2 months of walking, which have not been reported before. This can be explained as previous regional approaches in infancy considered the forefoot as whole, preventing detection of changes in discrete anatomical regions.

Keywords: pSPM, foot, plantar pressure, infants, gait

1. Introduction

Quantifying plantar pressure data as infants learn and master walking skills enhances knowledge of the typical biomechanics of the foot throughout development, providing information related to foot function changes. The conventional approach to analysis and reporting infants' pressure data is regional analysis, which has been adopted using three, five, six or seven regions of interest (ROIs) (Montagnani et al., 2021, in press). Traditional regional analysis software have been developed to be accessible without the need to understand programming languages (e.g., MATLAB, Python), making it easy to implement for pressure data processing. This ease in processing data comes with certain disadvantages, notably assumptions relating to the statistical treatment of regional data as discrete, treating the regions of the foot independently (Pataky and Goulermas, 2008). Furthermore, the use of regional analysis in infancy presents limitations due to the ongoing foot development, which causes lack of clear anatomical definition on the plantar surface and hypotheses relating to the ROIs typically analyzed in the plantar pressure field.

Pedobarographic Statistical Parametric Mapping (pSPM) conducts statistical inference at the pixel level in the spatial domain (Pataky and Goulermas, 2008), and it has been adopted in adults (McClymont et al., 2016; Oliveira et al., 2010; Pataky et al., 2008) and children (Phethean et al., 2014). However, the use of pSPM in infants' pressure analysis has not been reported. Adopting pSPM could be non-trivial in infancy, as foot placement on the pressure platform could be influenced by the combination of high variability in gait, the testing protocol adopted, and the developmental characteristics of the infant's feet. These factors lead to capturing steps highly irregular in shape and spatial orientation (Price et al., 2017) that could make data processing challenging. Therefore, this study aimed to detail the implementation of the pSPM processing framework on pressure data captured in infants. By undertaking this work, we also aimed to compare pressure patterns of new and confident walking infants, providing a preliminary set of novel information about plantar pressure patterns that could direct future research in the field.

2. Methods

This work emerges from a longitudinal study, which is part of the Great Foundation Initiative (Price et al., 2018). Ethical approval was obtained from the ethics committees of the Schools of Health Sciences at the University of Brighton (LHPSCREC 17-11) and the University of Salford (HSCR161779).

2. 1 Participants

Twelve infants (5 female, 7 males) were recruited via social media and local communities in the South East (Brighton) and North West (Salford) of England. Infants were born full-term, without neurological and/or musculoskeletal conditions, impairment in attaining walking stages or gross motor development deficiency. For data collection, infants came to the Human Movement Laboratory of the respective Universities at the attainment of two stages of foot loading (Price et al., 2018):

- New walking: infants able to take 3 to 5 steps independently: mean age (SD): 13.2 months (1.0); weight: 10.8 (1.1) kg; foot length: 11.4 (0.8) cm; foot width: 5.4 (0.4).
- Confident walking: infants able to take 10-15 steps independently and confidently, interacting with others, carrying toys while walking, navigating around objects: mean age (SD): 15.1 months (1.3); weight: 11.3 (1.2) kg; foot length: 12.0 (0.8) cm; foot width: 5.4 (0.5).

Once infants reached each stage, parents were asked to book the visit within 21 days. At each stage, written informed consent was given by parents.

2.2 Testing procedure

Plantar pressure data were collected using the EMED xl platform (4 sensors per cm^2, 100Hz; Novel, Munich, Germany), embedded in a nursery-style environment (Price et al., 2018). After familiarizing with the space, infants walked freely, in self-selected directions and speed, across the space, while HD video was collected (Vicon Bonita 720c; Oxford, U.K/Logitech HD Pro Webcam).

2.3 Data pre-processing pSPM framework

Steps were extracted from the pressure trials in the EMED software and processed if the feet were within the platform borders and did not miss extensive anatomical parts. Visual inspection of the stance phases was also performed to ensure processing of steps from full gait cycles. This was necessary due to the diverse nature of foot contact of new and confident walking steps. Left feet (LF) and right feet (RF) were processed and analyzed separately, assuming population-level asymmetry. Three steps for each foot, for each participant at each stage were used for this work (n=144). Maximum pressure pictures (MPPs) of the steps were exported as ASCII text files (Novel Emascii software), and imported into MATLAB 2019a (The Mathworks Inc, Natick, USA) as 2-dimensional (2D) numeric matrices for data processing and analysis. Each MPP was then positioned in a grid of 36x25 pixels, to standardize matrix dimensions of each MPP. Non-zero entries of the MPP matrices corresponded to pixels containing pressure values.

2.3.1 Transformation to point clouds

The coordinates of the pixels in the matrices' reference system were used to represent the pixels in the 3-dimensional (3D) Euclidian space. We used such representation to convert MPPs into point clouds using a built-in MATLAB function that transformed each pixel into a point, whilst pressure values within each pixel were stored in separate vectors.

2.3.2 Within-subjects registration

Point clouds were registered within subject (WS) to a chosen template, defined as the point cloud with the highest number of points. Point clouds that were subject to registration will be referred to as sources. To perform WS registration, a rigid iterative closest point (ICP) algorithm for point cloud registration was used (Besl and McKay, 1992), in the form of a built in MATLAB function. However, the visual inspection of the data highlighted highly variable shape and spatial orientation of the steps (Fig. 1). The ICP algorithm is highly susceptible to local minima and its performance relies on the quality of the initial pose of the point clouds with respect to the template (Yang et al., 2015). For this reason, previous works has tried to improve its implementation by performing initial coarse alignment of the data

(Makadia et al., 2006; Rusu et al., 2009). Therefore, an additional data processing passage was required prior to WS registration, to yield optimal points overlap. This was obtain by vertically aligning the original MPPs using principal component analysis (PCA), similarly to Kim et al. (2013).

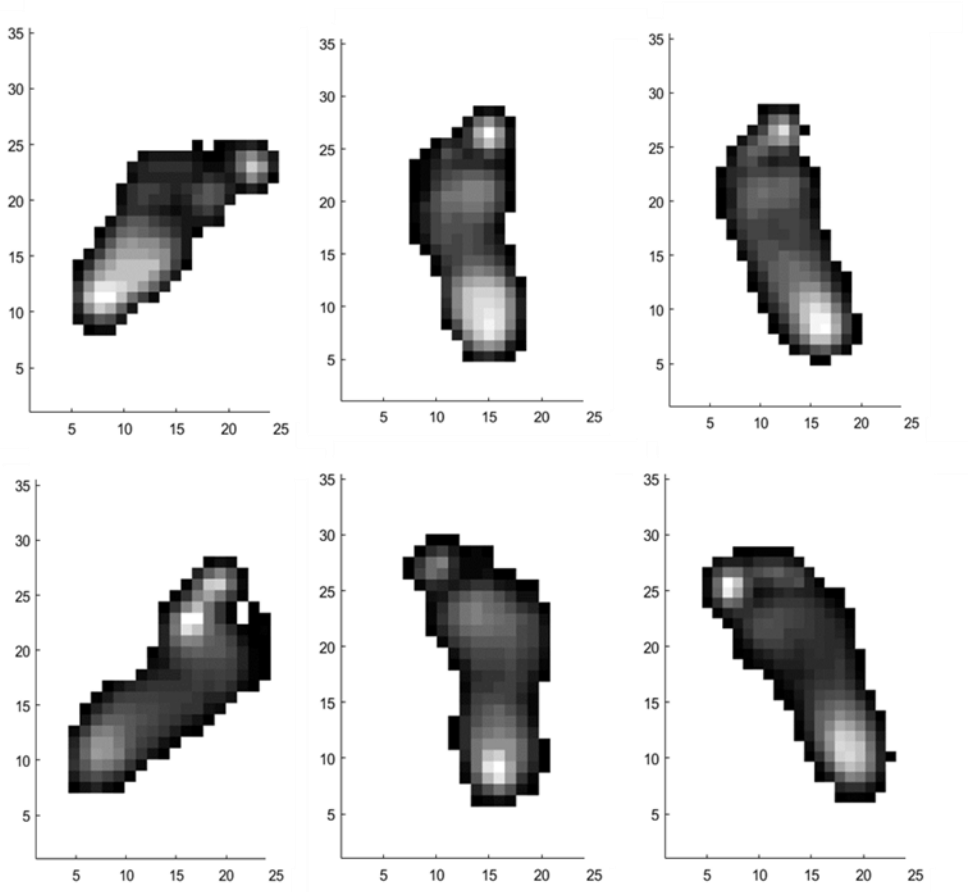

Fig. 1. Example of the spatial orientation of left and right MPPs positioned in a common reference system of 36x25 pixels.

2.3.3 Computing axes of MPPs using principal component analysis (PCA)

Binary MPPs were created and matrices of each MPP were put in two vectors (*a* and *b*) as coordinates. The means of *a* and *b* were calculated and subtracted from each index of the respective coordinates, creating new vectors: A and B. This enabled to find the centroid of the MPP. Vectors were positioned in a matrix, defining its columns. Covariance matrix was then calculated as:

$$C = \begin{pmatrix} cov\,(A,A) & cov\,(A,B) \\ cov(B,A) & cov\,(B,B) \end{pmatrix} \quad (1)$$

Eigenvectors and eigenvalues of the covariance matrix were found and plotted as the principal axes of the MPPs (Fig.2). To perform a counterclockwise rotation of the MPPs, Θ was calculated as the angle forming between the longest eigenvector (x_1) and the vector parallel (black dashed line) to the y-axis passing through the centroid (y_1) (Fig.2), according to:

$$\theta = atan(x_1, y_1) \quad (2)$$

Where *atan* is a built-in MATLAB function returning the inverse tangent ($\tan^{-1}$) of the ratio of x_1 and y_1 in radians. Once Θ was calculated (2), it was applied in the rotational transformation matrix (3), having the general form:

$$\begin{pmatrix} \cos\theta & -\sin\theta \\ \sin\theta & \cos\theta \end{pmatrix} \quad (3)$$

to enable counterclockwise rotation of the MPPs to vertical. Coordinates were then multiplied by the resulting transformation matrix, obtaining vertically aligned MPPs (Fig.2).

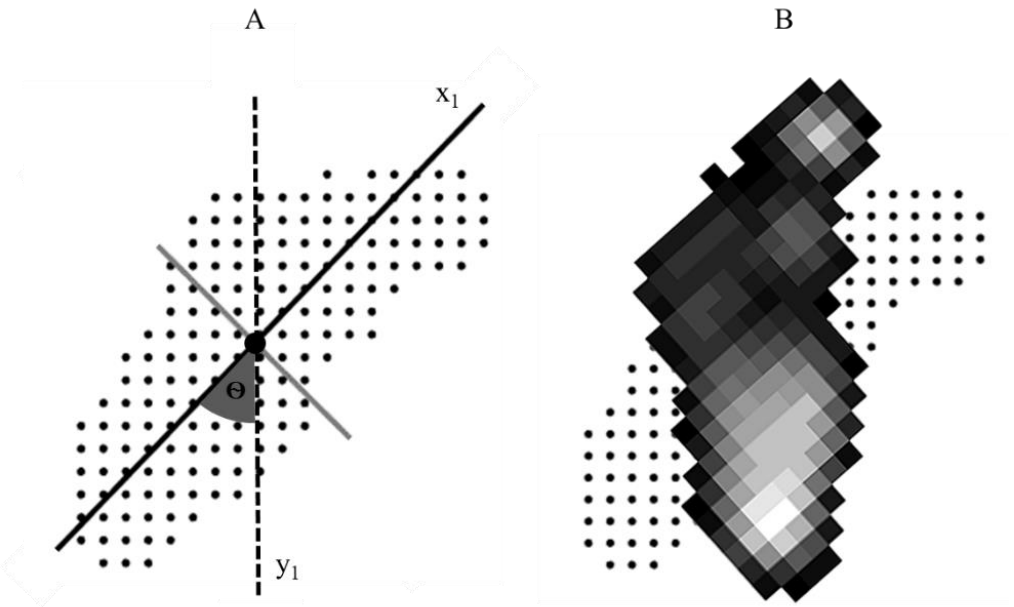

159

160 **Fig. 2.** (A) non-aligned MPP (black dots), principal axes are identified as black (x_1) and grey lines intersecting
161 at the image centroid, where the vector parallel to the y-axis passes through (y_1); x_1 and y_1 were used to
162 calculate Θ. The grey, shorter axis was reported for display purposes, enabling to visualize the centroid of the
163 MPP, thus the intersecting point of y_1. (B) Non-aligned binary MPP (black dots) and vertically aligned MPP
164 (greyscale, pixel-image).

165

166 Once PCA was performed, the rotated MPPs were re-transformed to point clouds, and WS registration
167 was achieved through the rigid ICP algorithm. Quality of WS registration pre and post PCA is also
168 reported (Fig.S1)

169 After WS registration, for each vertex of the template a built-in MATLAB function was used (based on
170 Euclidean distances) that returns the nearest neighbors of a query point in the input point cloud, to find
171 corresponding points between the sources and the WS template.

172 *2.3.4 Averaging*

173 Once aligned and registered, corresponding coordinates of point clouds were averaged, resulting in one
174 mean point cloud per participant per foot (Phethean et al., 2014). This was performed to reduce the

impact of differences in shape and dimensions of the point clouds (Fig. 1), and to enhance further steps of data processing.

2.3.5 Between-subjects template computation and registration

To perform between subjects (BS) registration, an unbiased BS template was chosen as the foot with length and width closest to the mean length and width of all the feet analyzed (Pataky et al., 2011). The non-rigid coherent point drift (CPD) algorithm for point cloud registration was performed through a built-in MATLAB function, to allow the shape of the point clouds to change using a displacement field as transformation. Next, the nearest neighbors of each vertex in the source point clouds were found in the unbiased BS template to establish points' correspondences.

2.4 Statistical analysis

To determine registration quality, the root-mean-square error (RMSE) was calculated between the source and the template (Pataky, 2012) for each step. RMSE values were transformed to mm and mean and standard deviation (SD) were reported. Graphic representations of the registration quality were also reported for both WS and BS registrations.

Analysis with SPM1D was conducted between sets of point clouds of new and confident walking steps. This was possible as pressure data was spatially aligned and nonparametric inference used (Pataky and Goulermas, 2008). Analysis was conducted using a two-tailed, nonparametric paired sample SPM1D t-test (http://www.spm1d.org/), with significance set as α=0.05. A t-value was calculated at each point of the point clouds, defining an SPM t curve. As nonparametric inference was used, multiple comparison corrections was performed using nonparametric permutation test, where the critical threshold was based on the maximum test statistic value across the entire domain (Pataky, 2012). If the SPM t-curve crossed this critical threshold (t critical) at any point, significant points were located (Pataky, 2012), reflecting that pressure in those points is significantly different between new and confident walking steps. However, SPM1D only supports critical test statistic calculation, thus cluster-specific p values were not available. Nonparametric linear regression was also performed between body weight (confounding variable) and plantar pressure at pixel level using SPM1D (Fig.S2).

3. Results

3.1 Within and between subject registration quality

With respect to registration accuracy, the mean (SD) RMSEs in the LF were 0.36 mm (0.09) and 0.39 mm (0.08) for WS and BS registration, respectively. In the RF, the mean (SD) RMSEs were 0.38 mm (0.06) and 0.37 mm (0.05) for WS and BS registration, respectively. Visual representation of the registration performances was also presented in Fig. 3.

Fig. 3 (A) demonstrated minimal non-overlapping points found on the lateral border of the heel and the medial border of the hallux. Considering the BS registration, non-overlapping points were present around the apex of the toes, around the foot periphery and between the heel and the midfoot (Fig. 3, B).

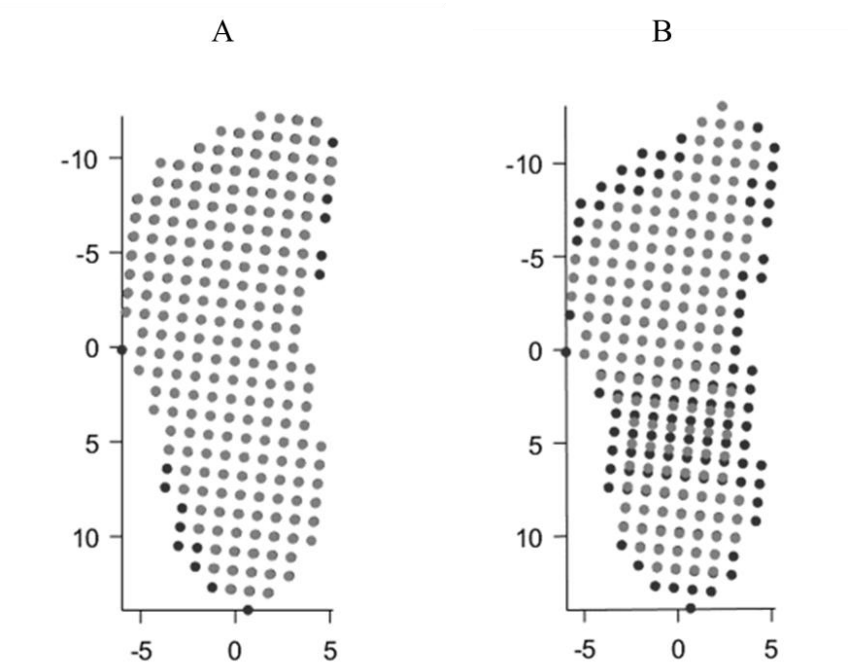

Fig. 3. Visual representation of the source (grey points) and template (black points) overlap during WS registration (A) and BS registration (B).

3.2 Plantar pressure inference

In the transition from new to confident walking, pSPM detected an area of significantly increasing pressure in the central forefoot of the LF (Fig. 4). Significant differences in pressures were not identified

in the RF; however, the qualitative trends suggested the presence of increased pressure in the central heel, medial to lateral forefoot and decreased in the hallux in both LF and RF (Fig. 4 and 5).

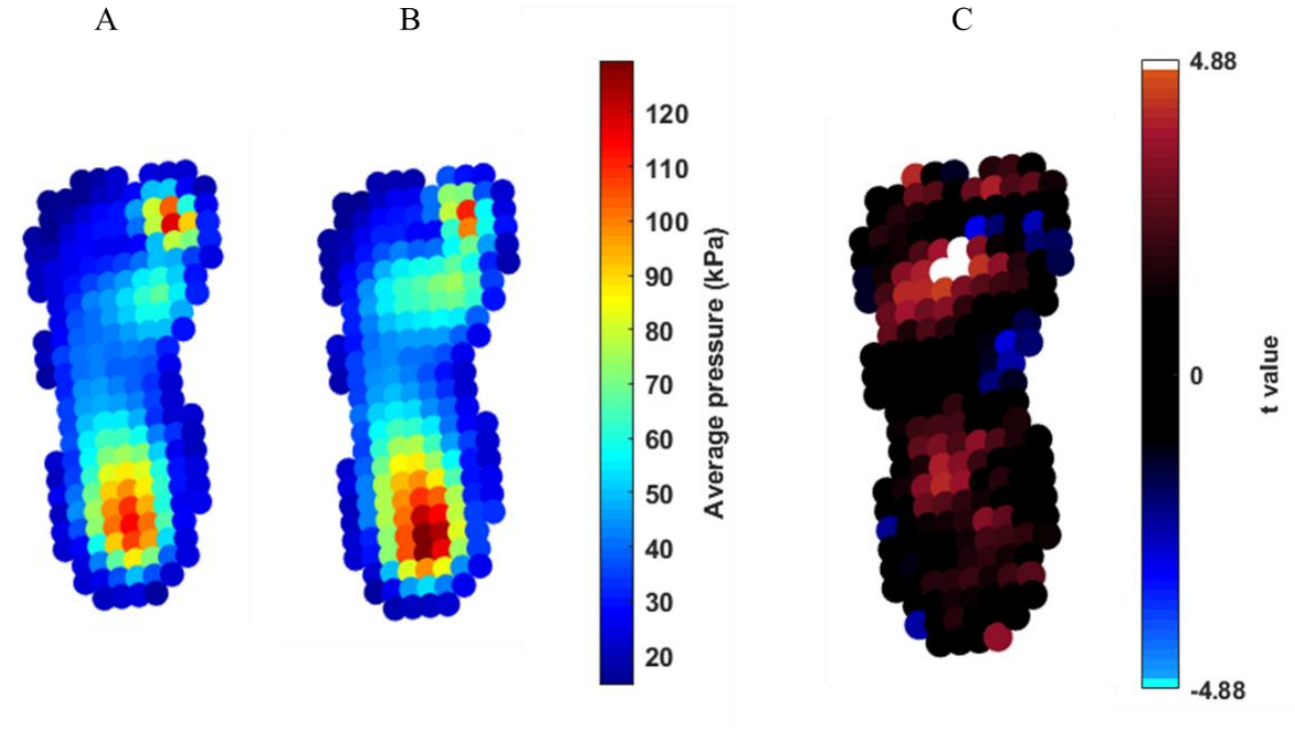

Fig. 4. Nonparametric pSPM paired t test on left feet for comparison between new and confident walking steps. From left to right: average pressure distribution of new walking (A), average pressure distribution of confident walking (B), and raw t value of statistical analysis (C), where the extremes of the colourbar reflects t-values needed to reach statistical significance, with alpha set at 0.05. The colourbar for A and B presented different min and max kPa values that were adjusted by the overall max and min values to allow for comparison. Cool and warm colours identify where confident walking steps had lower and higher peak pressure than new walking steps, respectively (C).

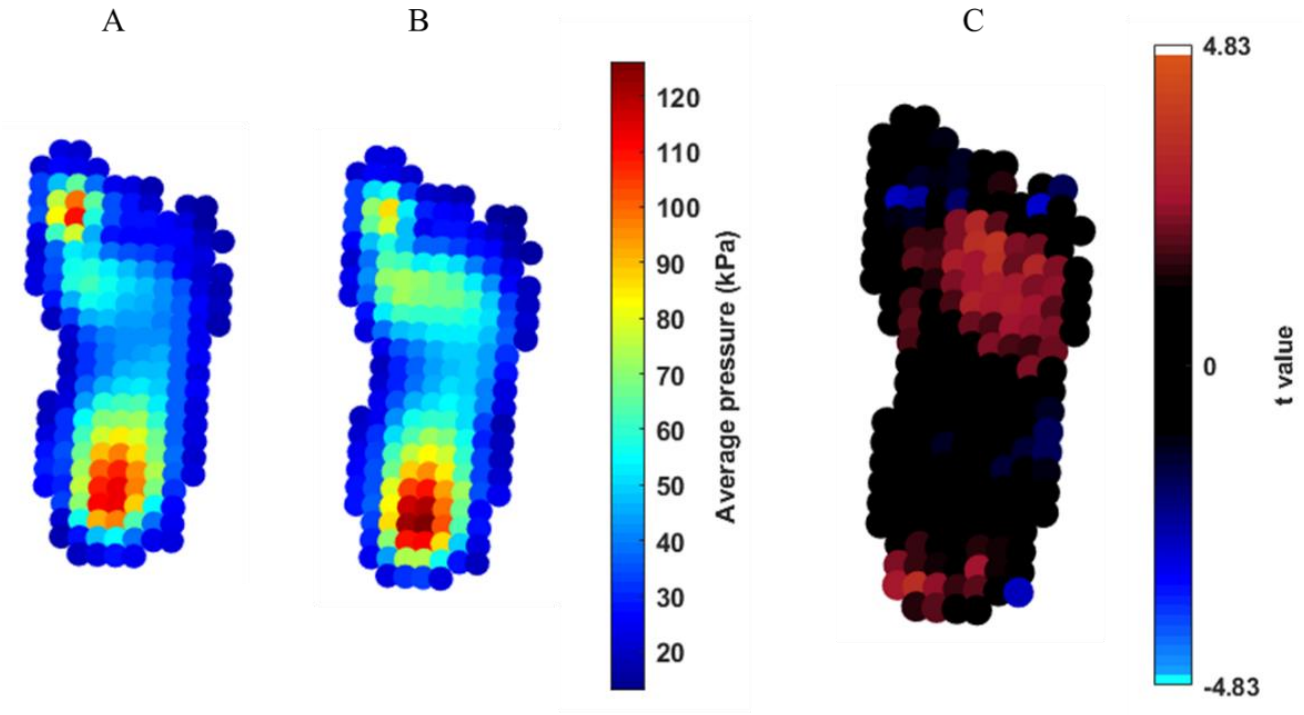

Fig. 5. Nonparametric pSPM paired t test on the right feet for comparison between new and confident walking steps. From left to right: average pressure distribution of new walking (A), average pressure distribution of confident walking (B), and raw t value of statistical analysis (C), where the extremes of the colourbar reflects t-values needed to reach statistical significance, with alpha set at 0.05. The colourbar for A and B presented different min and max kPa values that were adjusted by the overall max and min values to allow for comparison. Cool and warm colours identify where confident walking steps had lower and higher peak pressure than new walking steps, respectively (C).

Regression analysis of the pixel-level data revealed the absence of statistically significant correlation between the increasing body weight and plantar pressure in both feet (Fig.S2).

4. Discussion

This work reported details of the implementation of the pSPM approach to infants' pressure data, also investigating changes in plantar pressure as walking experience increases.

4.1 Methodological considerations

The use of pSPM in infancy is important to provide clear and unbiased insights into foot development. Traditional software for pressure data processing rely on the assumption that analysis is carried out on data presenting geometrical and/or pressure gradient patterns of adults' feet (Ellis et al., 2011). Although regional analysis is advantageous under certain circumstances (e.g., offloading specific foot regions), its use is debatable in the context of development, due to the ongoing anatomical and structural changes of the infants' feet. These changes prevent the foot from acting as a typically functional unit and therefore undermine the relevance of common ROI boundaries implemented in typically developed feet. Therefore, by selecting a methodology that divides the foot into ROIs according to adults' feet features, researchers imply that the infant foot is a well-developed functional unit, ignoring its anatomical and functional characteristics.

Another important methodological aspect of this study is the testing protocol and its effect on pressure data in infancy. Infants were able to walk freely and uninstructed as opposed to being restricted to a straight line, causing inconsistent directions of foot progression and contact patterns. Therefore, we anticipated the presence of a high intra, inter individual variability, and assumed the presence of population-level asymmetry in gait and related pressure patterns, which is why both feet were analyzed in this study.

The presence of intra and inter subject variability associated with the unrestrained testing protocol could also contribute to reduced registration quality. However, the rigid ICP algorithm, enhanced by PCA (Fig.S1), yielded low RMSEs in both LF and RF. This can be due to the closer intra-individual correspondences in feet dimensions. The quality of the WS registration was also shown in Fig. 3 (A), where the optimal overlap of points suggests a satisfying performance of the ICP algorithm to the present data set. Performance of CPD algorithm was slightly less accurate, considering the RMSE values and the visual representation of the registration (Fig. 3, B). This could be explained by the high inter-individual differences in foot dimensions and profile on the pressure platform. Nevertheless, RMSEs were under 0.4 mm for both WS and BS registration, which, considering the mean foot length and width, indicates good fit of the sources to the template. Moreover, the low SD reported in both registrations suggested that the ICP and CPD algorithms performed consistently on the point clouds,

without high between registration variations. These results suggest that the proposed methodology provided an effective, high quality, and solid framework to implement pSPM to free walking pressure data in infancy.

4.2 Functional considerations

This study suggests that after 2.2 months of independent walking experience, pressure significantly increases in the central left forefoot during gait. This has also been previously identified between 4 and 7 years, and authors argued about anatomical foot changes taking place (Phethean et al., 2014). In this work, anatomical foot development is unlikely to occur at a rate that would cause significant differences in pressure to happen, due to the short period between stages of foot loading (2.2 months). Furthermore, our analysis revealed that the increasing body weight did not influence plantar pressure data (Fig.S2). This could be due to the minimal increase in weight between new and confident walking stages (+0.5 kg; ~ 5% of initial body weight), which occurred alongside a corresponding ~5% increase in foot length. A previous comparison of infants (mean age: 23.5 (5.7) months) identified statistically increasing pressure in the central forefoot between trials of walking and running (Hennig and Rosenbaum, 1991). This could suggest that significant pressure changes in the central left forefoot could be attributed to the increasing walking speed, as infants become more experienced in walking. However, this was not quantified and reported as part of this research and would require further exploration.

Significant increase in pressure in the central forefoot between these stages of foot loading has not been reported in the literature before, and it could be due to different methodological approaches. Bertsch et al. (2004) found that during the first year of independent walking, the whole forefoot demonstrated significantly increasing pressure. However, the exact anatomical location of such change was unknown due to the application of a whole forefoot region. This implies that differences in pressure distribution could have been anywhere within the boundaries of the forefoot, limiting considerations regarding plantar pressure changes in the transition to confident walking. Increasing the resolution of the forefoot mask (e.g., lateral, central, and medial forefoot) might lead to the detection of significant differences in the central forefoot. However, statistical outcomes would be highly dependent on the ROI selected

(definition and number of ROIs), which causes arbitrary and inconsistent exploration of infants' pressure data, as reported elsewhere (Montagnani et al., 2021, in press).

Other changes in pressure were identified also qualitatively in both feet, and specifically in the central heel, medial to lateral forefoot and hallux (Fig. 4 and 5, A, B). Previous works demonstrated that pressure in the hallux is the highest during the first few months of independent walking but decreases after three to six months of walking (Bertsch et al., 2004; Bosch et al., 2010; Hennig and Rosenbaum, 1991). The literature also report significant increasing heel pressure during the first year of independent walking (Bertsch et al., 2004), as initial heel contact occurs as opposed to forefoot contact (Hallemans et al., 2003; Hallemans et al., 2006). Findings from our work agree with previous studies and suggest that changes in pressure occur rapidly, as infants become confident in walking. As opposed to previous works reporting data in infancy for either LF, RF, or mixed (Alvarez et al., 2008; Bertsch et al., 2004; Bosch et al., 2010), our work showed different statistical results in LF and RF. This could be the related to the presence of high inter-limb asymmetry during the first months of walking (Ledebt et al., 2004), which could lead to different pressure changes in the RF and LF between early and confident walking. However, because a large area of non-significant pressure increase is visible in the RF (Fig. 5), differences in statistical outcomes might in-fact be due to the small sample size analyzed, in terms of both the number of participants and steps included in the analysis. This could also explain why we were not able to detect larger areas of significant changes in pressure in either foot during the transition to confident walking. Combining pressure data from LF and RF by mirroring would have provided a larger sample size, but this would have assumed population-level symmetry in gait and related pressure patterns within the loading stages.

Thus, additional work should be undertaken to investigate whether differences in pressure are present between LF and RF within foot loading stages, which would illuminate population-level symmetry in plantar pressure patterns. Future research analyzing a larger sample with pSPM may have the capability to detect the presence of plantar pressure changes that have not been reported before. Therefore, further investigations with the present methodology are warranted, to increase resolution of data analysis and ensure clearer understanding of foot function development, as infants become confident in walking.

Acknowledgment

Dr. Stewart Morrison held the grant provided by The Dr William M Scholl Unit of Podiatric Development, which funded Dr. Carina Price, Matyas Varga and Eleonora Montagnani. At the time this article was written, Eleonora Montagnani and Matyas Varga were PhD students at the Department of Health Sciences at the University of Brighton, England.

References

Alvarez, C., De Vera, M., Chhina, H., Black, A., 2008. Normative data for the dynamic pedobarographic profiles of children. Gait Posture 28, 309-315.

Bertsch, C., Unger, H., Winkelmann, W., Rosenbaum, D., 2004. Evaluation of early walking patterns from plantar pressure distribution measurements. First year results of 42 children. Gait & Posture 19, 235-242.

Besl, P.J., McKay, N.D., Year Method for registration of 3-D shapes. In Sensor fusion IV: control paradigms and data structures.

Bosch, K., Gerss, J., Rosenbaum, D., 2010. Development of healthy children's feet--nine-year results of a longitudinal investigation of plantar loading patterns. Gait Posture 32, 564-571.

Ellis, S.J., Stoecklein, H., Yu, J.C., Syrkin, G., Hillstrom, H., Deland, J.T., 2011. The accuracy of an automasking algorithm in plantar pressure measurements. HSS Journal® 7, 57-63.

Hallemans, A., D'Août, K., De Clercq, D., Aerts, P., 2003. Pressure distribution patterns under the feet of new walkers: the first two months of independent walking. Foot & ankle international 24, 444-453.

Hallemans, A., De Clercq, D., Van Dongen, S., Aerts, P., 2006. Changes in foot-function parameters during the first 5 months after the onset of independent walking: a longitudinal follow-up study. Gait Posture 23, 142-148.

Hennig, E.M., Rosenbaum, D., 1991. Pressure distribution patterns under the feet of children in comparison with adults. Foot & ankle 11, 306-311.

345 Kim, C., Son, H., Kim, C., 2013. Fully automated registration of 3D data to a 3D CAD model for project
346 progress monitoring. Automation in Construction 35, 587-594.

347 Ledebt, A., van Wieringen, P.C., Savelsbergh, G.J., 2004. Functional significance of foot rotation
348 asymmetry in early walking. Infant Behavior and Development 27, 163-172.

349 Makadia, A., Patterson, A., Daniilidis, K., Year Fully automatic registration of 3D point clouds. In 2006
350 IEEE Computer Society Conference on Computer Vision and Pattern Recognition (CVPR'06).

351 Montagnani, E., Price, C., Nester, C., Morrison, SC., 2021. Dynamic Characteristics of Foot
352 Development: A Narrative Synthesis of Plantar Pressure Data During Infancy and Childhood. Pediatric
353 Physical Therapy, doi: 10.1097/PEP.0000000000000819

354 McClymont, J., Pataky, T.C., Crompton, R.H., Savage, R., Bates, K.T., 2016. The nature of functional
355 variability in plantar pressure during a range of controlled walking speeds. Royal Society open science
356 3, 160369.

357 Oliveira, F.P., Pataky, T.C., Tavares, J.M.R., 2010. Registration of pedobarographic image data in the
358 frequency domain. Computer methods in biomechanics and biomedical engineering 13, 731-740.

359 Pataky, T.C., 2012. Spatial resolution in plantar pressure measurement revisited. Journal of
360 biomechanics 45, 2116-2124.

361 Pataky, T.C., Bosch, K., Mu, T., Keijsers, N.L., Segers, V., Rosenbaum, D., Goulermas, J.Y., 2011. An
362 anatomically unbiased foot template for inter-subject plantar pressure evaluation. Gait Posture 33, 418-
363 422.

364 Pataky, T.C., Caravaggi, P., Savage, R., Parker, D., Goulermas, J.Y., Sellers, W.I., Crompton, R.H.,
365 2008. New insights into the plantar pressure correlates of walking speed using pedobarographic
366 statistical parametric mapping (pSPM). Journal of biomechanics 41, 1987-1994.

367 Pataky, T.C., Goulermas, J.Y., 2008. Pedobarographic statistical parametric mapping (pSPM): a pixel-
368 level approach to foot pressure image analysis. Journal of biomechanics 41, 2136-2143.

Phethean, J., Pataky, T.C., Nester, C.J., Findlow, A.H., 2014. A cross-sectional study of age-related changes in plantar pressure distribution between 4 and 7 years: a comparison of regional and pixel-level analyses. Gait Posture 39, 154-160.

Price, C., McClymont, J., Hashmi, F., Morrison, S.C., Nester, C., 2018. Development of the infant foot as a load bearing structure: study protocol for a longitudinal evaluation (the Small Steps study). J Foot Ankle Res 11, 33.

Price, C., Morrison, S.C., Nester, C., 2017. Variability in foot contact patterns in independent walking in infants. Footwear Science 9, S47-S49.

Rusu, R.B., Blodow, N., Beetz, M., Year Fast point feature histograms (FPFH) for 3D registration. In 2009 IEEE international conference on robotics and automation.

Yang, J., Li, H., Campbell, D., Jia, Y., 2015. Go-ICP: A globally optimal solution to 3D ICP point-set registration. IEEE transactions on pattern analysis and machine intelligence 38, 2241-2254.

Supplementary figures

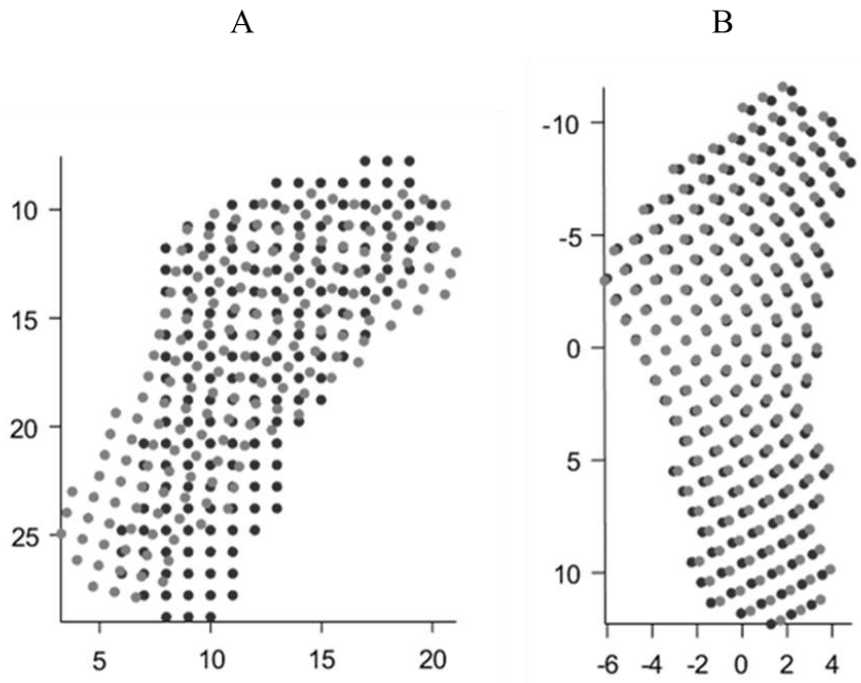

Fig. S1. Visual representation of WS registration performed without PCA (A) and with PCA (B).

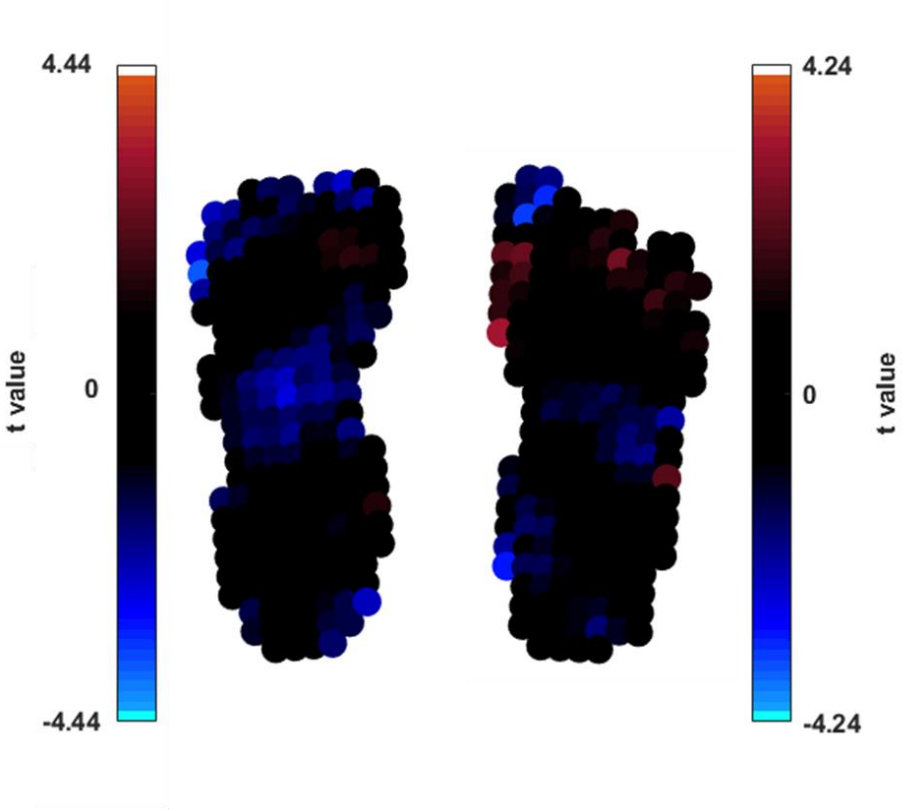

Fig. S2. Nonparametric linear regression analysis at pixel level, computed in both LF and RF. T-values indicates the strength of linear regression between increasing body weight and plantar pressure data.